Lissajous sampling and adaptive spectral filtering for the reduction of the Gibbs phenomenon in Magnetic Particle Imaging (MPI)

S. De Marchi[1], W. Erb[2] and F. Marchetti[1]

[1]University of Padova

[2]University of Hawaii

Bernried, 27 Feb. - 3 Mar. 2017

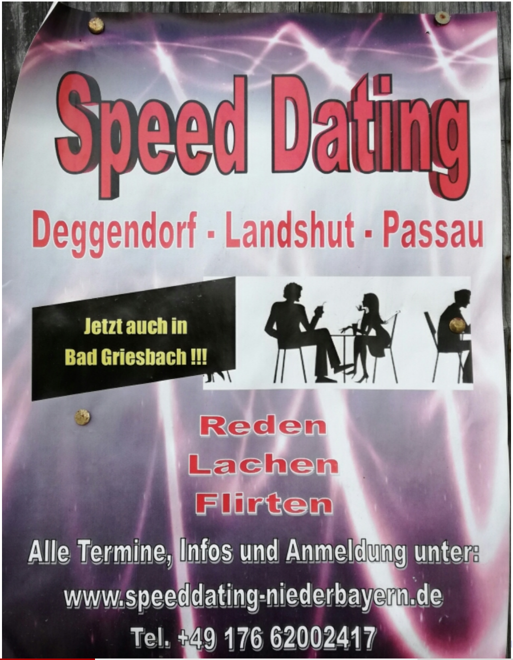
Speed Dating
Deggendorf - Landshut - Passau
Jetzt auch in
Bad Griesbach !!!
Reden
Lachen
Flirten
Alle Termine, Infos und Anmeldung unter:
www.speeddating-niederbayern.de
Tel. +49 176 62002417

Starting points

1. Padua points lie on a Lissajous curve [Bos, De Marchi et al. JAT 2006]

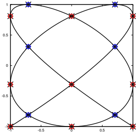

2. Magnetic Particle Imaging: *"The trajectory of the field-free point (FFP) describes a Lissajous curve"* [Weizenecker et al., Phy. in Med. 2007]

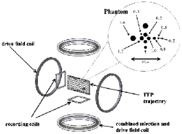

3. Reconstruction of discontinuos and piecewise regular functions by trun.

Fourier series $\rightsquigarrow$ Gibbs phenomenon 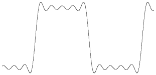 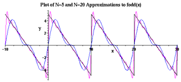

Outline

Magnetic Particle Imaging

Magnetic Particle Imaging (MPI)

The MPI is an emerging technology in the (pre)clinical imaging [B. Gleich, J. Weizenecker (Philips Research, Hamburg) - Nature 2005].

- Detection of a tracer consisting of super-paramagnetic (iron oxide) nanoparticles injected in the bloodstream ($\rightsquigarrow$ emissive tomography)
- 3D *Field of View* with high sensitivity, high resolution ($\sim$ 0.4mm) and high imaging speed ($\sim$ 20 ms)
- The acquisition of the signal, which comes from the particles, is performed moving a field-free point (FFP) along trajectories: (Lissajous curves)
- No radiation, no iodine, no background noise (high contrast).
- 1000 times faster than PET; 100 times more sensitive than MRI.

MPI scanners topologies

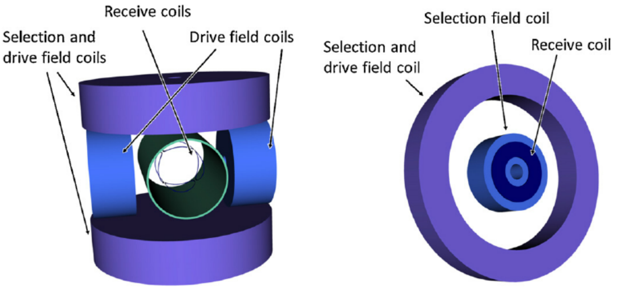

(a) MPI scanner with a cylindrical bore

(b) Single-sided scanner

Figure: Left: two pairs of transmit coils and two pairs of receivers coils. Right: one sided from IMT Lübeck

- Two-two scanner: the design imposes size limitation on the object
- One side: the target no longer has to be small enough to fit inside the scanner

MPI scanners

Figure: Left: scanner for humans. Right: the “Bruker-Philips BioSpin MPI” for animals

Lissajous curves

Bowditch figures or Lissajous curves

1. Are planar parametric curves studied by Nathaniel Bowditch (1815) and Jules A. Lissajous (1857) of the form

$$\gamma(t) = \left(A_x \cos(\omega_x t + \alpha_x), A_y \sin(\omega_y t + \alpha_y)\right).$$

A_x, A_y are amplitudes, ω_x, ω_y are pulsations and α_x, α_y are phases.

2. Chebyshev polynomials (T_k or U_k) are Lissajous curves (cf. J. C. Merino 2003). In fact a parametrization of $y = T_n(x)$, $|x| \le 1$ is

$$\begin{cases} x = \cos t \\ y = -\sin\left(nt - \frac{\pi}{2}\right) \quad 0 \le t \le \pi \end{cases}$$

Bowditch figures or Lissajous curves

1. Are planar parametric curves studied by Nathaniel Bowditch (1815) and Jules A. Lissajous (1857) of the form

$$\gamma(t) = (A_x \cos(\omega_x t + \alpha_x), A_y \sin(\omega_y t + \alpha_y)) .$$

A_x, A_y are amplitudes, ω_x, ω_y are pulsations and α_x, α_y are phases.

2. Chebyshev polynomials (T_k or U_k) are Lissajous curves (cf. J. C. Merino 2003). In fact a parametrization of $y = T_n(x)$, $|x| \leq 1$ is

$$\begin{cases} x = \cos t \\ y = -\sin\left(nt - \frac{\pi}{2}\right) \quad 0 \leq t \leq \pi \end{cases}$$


Figure: Left: N. Bowditch (March 26, 1773 - March 16, 1838), American mathematician remembered for his work on ocean navigation. Right: J. Lissajous (March 4, 1822 - June 24, 1880), French physicist

Two dimensional general definition [Erb et al. DRNA2015]

Definition

$$\gamma^{\boldsymbol{n}}_{\boldsymbol{\kappa},\boldsymbol{u}}(t) = \begin{pmatrix} u_1 \cos(n_2 t - \kappa_1 \pi/(2n_1)) \\ u_2 \cos(n_1 t - \kappa_2 \pi/(2n_2)) \end{pmatrix}, \; t \in [0, 2\pi],$$

with $\boldsymbol{n} = (n_1, n_2) \in \mathbb{N}^2$, $\boldsymbol{\kappa} = (\kappa_1, \kappa_2) \in \mathbb{R}^2$ and $\boldsymbol{u} = \{-1, 1\}^2$.

n_1, n_2 are called frequencies (like for the pendulum) and $\boldsymbol{u}$ reflection parameter.

Proposition

There exist $t' \in \mathbb{R}$, $\eta \in [0, 2)$ and $\boldsymbol{u}' \in \{-1, 1\}^2$ s.t.

$$\gamma^{\boldsymbol{n}}_{\boldsymbol{\kappa},\boldsymbol{u}}(t - t') := \gamma^{\boldsymbol{n}}_{(0,\eta),\boldsymbol{u}'}(t)\,, \; t \in [0, 2\pi] \quad (1)$$

Obs: if $\boldsymbol{\kappa} \in \mathbb{Z}^2$, the value of η can be always chosen as $\{0, 1\}$.

Two dimensional general definition [Erb et al. DRNA2015]

Definition

$$\gamma^{\boldsymbol{n}}_{\boldsymbol{\kappa},\boldsymbol{u}}(t) = \begin{pmatrix} u_1 \cos(n_2 t - \kappa_1 \pi/(2n_1)) \\ u_2 \cos(n_1 t - \kappa_2 \pi/(2n_2)) \end{pmatrix}, \; t \in [0, 2\pi],$$

with $\boldsymbol{n} = (n_1, n_2) \in \mathbb{N}^2$, $\boldsymbol{\kappa} = (\kappa_1, \kappa_2) \in \mathbb{R}^2$ and $\boldsymbol{u} = \{-1, 1\}^2$.

n_1, n_2 are called frequencies (like for the pendulum) and $\boldsymbol{u}$ reflection parameter.

Proposition

There exist $t' \in \mathbb{R}$, $\eta \in [0, 2)$ *and* $\boldsymbol{u}' \in \{-1, 1\}^2$ *s.t.*

$$\gamma^{\boldsymbol{n}}_{\boldsymbol{\kappa},\boldsymbol{u}}(t - t') := \gamma^{\boldsymbol{n}}_{(0,\eta),\boldsymbol{u}'}(t)\,, \; t \in [0, 2\pi] \tag{1}$$

Obs: if $\boldsymbol{\kappa} \in \mathbb{Z}^2$, the value of η can be always chosen as $\{0, 1\}$.

Lissajous curves (cont')

Lissajous curves on the square

Let $\boldsymbol{n} = (n_1, n_2)$ with $n_1, n_2 \in \mathbb{N}$ relatively primes. Then we can consider the parametric curves $\gamma_\epsilon^{\boldsymbol{n}} : [0, 2\pi] \to [-1, 1]^2$

$$\gamma_\epsilon^{\boldsymbol{n}}(t) := \gamma_{(0,\epsilon-1),\mathbf{1}}^{\boldsymbol{n}}(t) = \begin{pmatrix} \cos(n_2 t) \\ \cos(n_1 t + (\epsilon - 1)\pi/(2n_2)) \end{pmatrix} \tag{2}$$

with $\epsilon \in \{1, 2\}$ and fixed reflection parameter $\mathbf{1} = (1, 1)$.

Special cases

- $\epsilon = 1$ (i.e. $\eta = 0$ in (1) and $I = [0, \pi]$), $\gamma_1^{\boldsymbol{n}}(t)$ is called a degenerate curve [Erb AMC2016]
- $\epsilon = 2$ the curve is called non-degenerate [Erb et al. NM2016].

Lissajous curves (cont')

Lissajous curves on the square

Let $\boldsymbol{n} = (n_1, n_2)$ with $n_1, n_2 \in \mathbb{N}$ relatively primes. Then we can consider the parametric curves $\gamma_\epsilon^{\boldsymbol{n}} : [0, 2\pi] \to [-1, 1]^2$

$$\gamma_\epsilon^{\boldsymbol{n}}(t) := \gamma_{(0,\epsilon-1),\mathbf{1}}^{\boldsymbol{n}}(t) = \begin{pmatrix} \cos(n_2 t) \\ \cos(n_1 t + (\epsilon - 1)\pi/(2n_2)) \end{pmatrix} \tag{2}$$

with $\epsilon \in \{1, 2\}$ and fixed reflection parameter $\mathbf{1} = (1, 1)$.

Special cases

- $\epsilon = 1$ (i.e. $\eta = 0$ in (1) and $I = [0, \pi]$), $\gamma_1^{\boldsymbol{n}}(t)$ is called a degenerate curve [Erb AMC2016]
- $\epsilon = 2$ the curve is called non-degenerate [Erb et al. NM2016].

The Lissajous (node) points

Lissajous nodes

Let $\gamma_\epsilon^{\boldsymbol{n}}$ be a Lissajous curve with $\epsilon \in \{1, 2\}$ and let

$$t_k^{\epsilon \boldsymbol{n}} = \frac{\pi k}{\epsilon n_1 n_2}\,, \quad k = 0, \ldots, 2\epsilon n_1 n_2 - 1\ .$$

The set

$$LS_\epsilon^{\boldsymbol{n}} = \{\gamma_\epsilon^{\boldsymbol{n}}(t_k^{\epsilon \boldsymbol{n}}) : \quad k = 0, \ldots, 2\epsilon n_1 n_2 - 1\}$$

is the set of Lissajous node points related to $\gamma_\epsilon^{\boldsymbol{n}}$.

We need also to introduce the set of indices

$$\Gamma^{\epsilon \boldsymbol{n}} = \left\{(i, j) \in \mathbb{N}_0^2 \ : \ \frac{i}{\epsilon n_1} + \frac{j}{\epsilon n_2} < 1\right\} \cup \{(0, \epsilon n_2)\}\ .$$

Examples

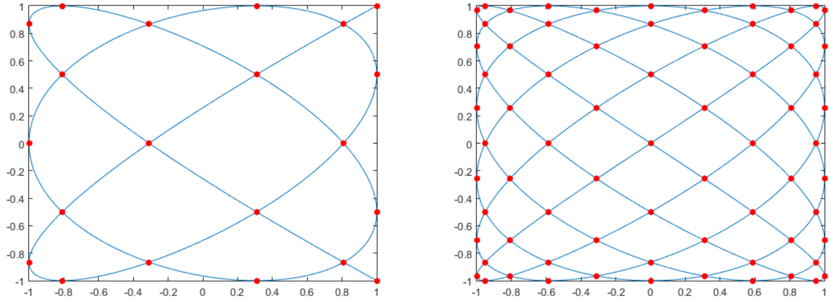

Figure: plots of $\gamma_1^{(5,6)}$ and $\gamma_2^{(5,6)}$

$$\#LS_1^{(5,6)} = 21 = \dim\Pi_5^2 = \#PD_5, \quad \#LS_2^{(5,6)} = 71 < \dim\Pi_{11}^2 = 78$$

$$\#LS_\epsilon^{\boldsymbol{n}} = \#\Gamma^{\epsilon\boldsymbol{n}} = \frac{(\epsilon n_1+1)(\epsilon n_2+1)-(\epsilon-1)}{2} \tag{3}$$

Padua and Morrow-Patterson points

Padua points correspond to the degenerate Lissajous curve (cf. (2)) $\gamma_{\mathbf{0},\boldsymbol{u}}^{(n,n+1)}$ or $\gamma_{\mathbf{0},\boldsymbol{u}}^{(n+1,n)}$, $n \in \mathbb{N}$.
Up to reflection $\boldsymbol{u}$, they are given by the curves

$$\gamma_1^{\boldsymbol{n}}(t) = \begin{pmatrix} \cos nt \\ \cos(n+1)t \end{pmatrix} \text{ or } \gamma_1^{\boldsymbol{n}}(t) = \begin{pmatrix} \cos(n+1)t \\ \cos nt \end{pmatrix}.$$

The Morrow-Patterson come from $\gamma_1^{(n+2,n+3)}$ which are the self-intersection points of the Padua's curve $\gamma_1^{(n,n+1)}$.

Padua and Morrow-Patterson points

Padua points correspond to the degenerate Lissajous curve (cf. (2)) $\gamma_{\mathbf{0},\boldsymbol{u}}^{(n,n+1)}$ or $\gamma_{\mathbf{0},\boldsymbol{u}}^{(n+1,n)}$, $n \in \mathbb{N}$.
Up to reflection $\boldsymbol{u}$, they are given by the curves

$$\gamma_1^{\boldsymbol{n}}(t) = \begin{pmatrix} \cos nt \\ \cos(n+1)t \end{pmatrix} \text{ or } \gamma_1^{\boldsymbol{n}}(t) = \begin{pmatrix} \cos(n+1)t \\ \cos nt \end{pmatrix}.$$

The Morrow-Patterson come from $\gamma_1^{(n+2,n+3)}$ which are the self-intersection points of the Padua's curve $\gamma_1^{(n,n+1)}$.

Padua pts and MP pts

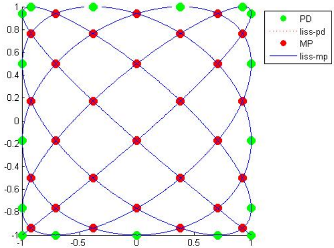

Figure: Padua and MP points for $n = 6$ or $\boldsymbol{n} = (6, 7)$

- In [Bos,DeM,Vianello,Xu JAT2006]: $\#PD_n = \binom{n+2}{2}$, unisolvent set for polynomial interpolation of total degree on $[-1,1]^2$ and $\Lambda_{PD_n} = \mathcal{O}(\log^2 n)$
- In [DeM Vianello, DRNA 7, 2014] : $\Lambda_{MP_n} = \mathcal{O}(n^3)$ while numerical growth is $\mathcal{O}(n^2)$.

Padua pts and MP pts

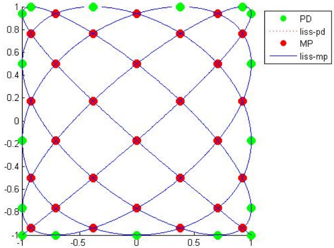

Figure: Padua and MP points for $n = 6$ or $\boldsymbol{n} = (6, 7)$

- In [Bos,DeM,Vianello,Xu JAT2006]: $\#PD_n = \binom{n+2}{2}$, unisolvent set for polynomial interpolation of total degree on $[-1, 1]^2$ and $\Lambda_{PD_n} = \mathcal{O}(\log^2 n)$
- In [DeM Vianello, DRNA 7, 2014] : $\Lambda_{MP_n} = \mathcal{O}(n^3)$ while numerical growth is $\mathcal{O}(n^2)$.

Polynomial space

We consider the polynomial space on $[-1,1]^2$

$$\Pi^{\epsilon \boldsymbol{n}} = \mathrm{span}\{\hat{\phi}_{i,j}(\boldsymbol{x}) \, : \, (i,j) \in \Gamma^{\epsilon \boldsymbol{n}}\} \, ,$$

with $\boldsymbol{x} = (x_1, x_2)$

$$\hat{\phi}_{i,j}(\boldsymbol{x}) = \hat{T}_i(x_1)\hat{T}_j(x_2)$$

$\hat{T}_0(x_1) = 1$ and $\hat{T}_i(x_1) = \sqrt{2}\cos(i \arccos x_1))$ the i-th normalized Chebyshev polynomial of the first kind.

As well known is an orthogonal basis of $\Pi^{\epsilon \boldsymbol{n}}$ w.r.t. the inner product

$$\langle f, g \rangle = \frac{1}{\pi^2} \int_{-1}^{1} \int_{-1}^{1} f(x,y) g(x,y) \omega(x,y) \mathrm{d}x \mathrm{d}y$$

and the product measure $\omega(x,y) = \frac{1}{\sqrt{1-x^2}} \frac{1}{\sqrt{1-y^2}}$.

Polynomial space

We consider the polynomial space on $[-1,1]^2$

$$\Pi^{\epsilon \boldsymbol{n}} = \mathrm{span}\{\hat{\phi}_{i,j}(\boldsymbol{x}) \,:\, (i,j) \in \Gamma^{\epsilon \boldsymbol{n}}\} \ ,$$

with $\boldsymbol{x} = (x_1, x_2)$

$$\hat{\phi}_{i,j}(\boldsymbol{x}) = \hat{T}_i(x_1)\hat{T}_j(x_2)$$

$\hat{T}_0(x_1) = 1$ and $\hat{T}_i(x_1) = \sqrt{2}\cos(i \arccos x_1))$ the i-th normalized Chebyshev polynomial of the first kind.
As well known is an orthogonal basis of $\Pi^{\epsilon \boldsymbol{n}}$ w.r.t. the inner product

$$\langle f, g\rangle = \frac{1}{\pi^2}\int_{-1}^{1}\int_{-1}^{1} f(x,y)g(x,y)\omega(x,y)\mathrm{d}x\mathrm{d}y$$

and the product measure $\omega(x,y) = \frac{1}{\sqrt{1-x^2}}\frac{1}{\sqrt{1-y^2}}$.

Interpolation on Lissajous nodes

[Erb et al. DRNA2015]: the unique polynomial interpolant $\mathcal{L}^{\epsilon\boldsymbol{n}} f$ in the space $\Pi^{\epsilon\boldsymbol{n}}$ of a given function f is

$$\mathcal{L}^{\epsilon\boldsymbol{n}} f(\boldsymbol{x}) = \sum_{(i,j)\in\Gamma^{\epsilon\boldsymbol{n}}} c_{ij}(f)\hat{\phi}_{i,j}(\boldsymbol{x})\,, \tag{4}$$

where the coefficients $c_{ij}(f)$ are uniquely given by the values of the function f on the point set $LS_{\epsilon}^{\boldsymbol{n}}$.

Using the change of variables $x = \cos(t)$, $y = \cos(s)$, and expanding the set $\Gamma^{\epsilon\boldsymbol{n}}$ in

$$\Gamma_S^{\epsilon\boldsymbol{n}} = \left\{(i,j)\in\mathbb{Z}^2\ :\ (|i|,|j|)\in\Gamma^{\epsilon\boldsymbol{n}}\right\}.$$

we can express the interpolant $\mathcal{L}^{\epsilon\boldsymbol{n}} f$ as the Fourier series

$$\mathcal{L}^{\epsilon\boldsymbol{n}} f(t,s) = \sum_{(i,j)\in\Gamma_S^{\epsilon\boldsymbol{n}}} \tilde{c}_{ij}\, e_i(t)e_j(s)\,,\ \ e_j(s) = e^{\mathrm{i}\,js}. \tag{5}$$

Interpolation on Lissajous nodes

[Erb et al. DRNA2015]: the unique polynomial interpolant $\mathcal{L}^{\epsilon \boldsymbol{n}} f$ in the space $\Pi^{\epsilon \boldsymbol{n}}$ of a given function f is

$$\mathcal{L}^{\epsilon \boldsymbol{n}} f(\boldsymbol{x}) = \sum_{(i,j) \in \Gamma^{\epsilon \boldsymbol{n}}} c_{ij}(f) \hat{\phi}_{i,j}(\boldsymbol{x}) \, , \tag{4}$$

where the coefficients $c_{ij}(f)$ are uniquely given by the values of the function f on the point set $LS_{\epsilon}^{\boldsymbol{n}}$.

Using the change of variables $x = \cos(t)$, $y = \cos(s)$, and expanding the set $\Gamma^{\epsilon \boldsymbol{n}}$ in

$$\Gamma_S^{\epsilon \boldsymbol{n}} = \left\{ (i,j) \in \mathbb{Z}^2 \; : \; (|i|, |j|) \in \Gamma^{\epsilon \boldsymbol{n}} \right\} .$$

we can express the interpolant $\mathcal{L}^{\epsilon \boldsymbol{n}} f$ as the Fourier series

$$\mathcal{L}^{\epsilon \boldsymbol{n}} f(t,s) = \sum_{(i,j) \in \Gamma_S^{\epsilon \boldsymbol{n}}} \tilde{c}_{ij} \, e_i(t) e_j(s) \, , \quad e_j(s) = e^{\mathrm{i} \, j s} \, . \tag{5}$$

Three-dimensional Lissajous curves

Given $\boldsymbol{a} = (a_1, a_2, a_3) \in \mathbb{N}^3$, we consider the curve in the cube $[-1, 1]^3$ defined as

$$\gamma_{\boldsymbol{a}}(t) = (\cos(a_1 t), \cos(a_2 t), \cos(a_3 t)) \ ,$$

where $t \in [0, \pi]$.

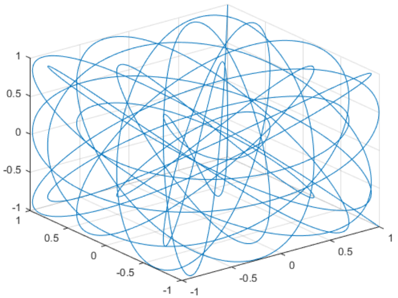

Figure: The curve $\gamma_{30,33,37}(t) = (\cos(30t), \cos(33t), \cos(37t))$.

Admissible triples

Definition

Let $V = \mathbb{P}_m^3$ be the space of trivariate polynomials of total degree $\leq m$ and let $\boldsymbol{a} = (a_1, a_2, a_3) \in \mathbb{N}^3$.
We say that $\boldsymbol{a}$ is V-admissible (of order m) if

$$\nexists\, \mathbf{0} \neq \boldsymbol{b} \in \mathbb{Z}^3 \ , \ |\boldsymbol{b}| = |b_1| + |b_2| + |b_3| \leq m \ ,$$

such that

$$a_1 b_1 + a_2 b_2 + a_3 b_3 = 0 \ .$$

We call $\mathcal{A}(V)$ the set of such admissible triples.

Fundamental theorem [Bos,DeM,Vianello IMA J.NA 2017]

This results shows which are the admissible 3d-Lissajous curves

Theorem

Let $n \in \mathbb{N}^+$ and (a_1, a_2, a_3) be the integer triple

$$(a_1, a_2, a_3) = \begin{cases} \left(\frac{3}{4}n^2 + \frac{1}{2}n, \frac{3}{4}n^2 + n, \frac{3}{4}n^2 + \frac{3}{2}n + 1\right)\ , & n \text{ even} \\ \left(\frac{3}{4}n^2 + \frac{1}{4}, \frac{3}{4}n^2 + \frac{3}{2}n - \frac{1}{4}, \frac{3}{4}n^2 + \frac{3}{2}n + \frac{3}{4}\right)\ , & n \text{ odd.} \end{cases} \tag{6}$$

Then, for every integer triple (i, j, k), not all 0, with $i, j, k \geq 0$ and $i + j + k \leq 2n$, we have the property that $ia_1 \neq ja_2 + ka_3$, $ja_2 \neq ia_1 + ka_3$, $ka_3 \neq ia_1 + ja_2$.
Moreover, $2n$ is maximal, in the sense that there exists a triple (i^*, j^*, k^*), $i^* + j^* + k^* = 2n + 1$, that does not satisfy the property.

Conjecture: the triples (6) are optimal,

$$\boxed{\min_{\mathbf{a} \in \mathcal{A}(V)} \max_{1 \leq i \leq 3} a_i = \mathcal{O}(n^2)\,.}$$

Fundamental theorem [Bos,DeM,Vianello IMA J.NA 2017]

This results shows which are the admissible 3d-Lissajous curves

Theorem

Let $n \in \mathbb{N}^+$ and (a_1, a_2, a_3) be the integer triple

$$(a_1, a_2, a_3) = \begin{cases} \left(\frac{3}{4}n^2 + \frac{1}{2}n, \frac{3}{4}n^2 + n, \frac{3}{4}n^2 + \frac{3}{2}n + 1\right), & n \text{ even} \\ \left(\frac{3}{4}n^2 + \frac{1}{4}, \frac{3}{4}n^2 + \frac{3}{2}n - \frac{1}{4}, \frac{3}{4}n^2 + \frac{3}{2}n + \frac{3}{4}\right), & n \text{ odd.} \end{cases} \quad (6)$$

Then, for every integer triple (i, j, k), not all 0, with $i, j, k \geq 0$ and $i + j + k \leq 2n$, we have the property that $ia_1 \neq ja_2 + ka_3$, $ja_2 \neq ia_1 + ka_3$, $ka_3 \neq ia_1 + ja_2$.
Moreover, $2n$ is maximal, in the sense that there exists a triple (i^*, j^*, k^*), $i^* + j^* + k^* = 2n + 1$, that does not satisfy the property.

Conjecture: the triples (6) are optimal,

$$\boxed{\min_{\mathbf{a} \in \mathcal{A}(V)} \max_{1 \leq i \leq 3} a_i = \mathcal{O}(n^2)\,.}$$

“Optimal” triples obtained by computer search

m	triples		
2	1	2	3
3	1	3	5
	3	4	5
4	4	5	7
	4	6	7
5	7	8	10
	7	9	10
6	7	11	12
7	7	15	17
	9	11	17
	9	15	17
	10	16	17
	13	14	17
	13	16	17
8	14	16	19
	14	17	19
9	19	21	24
	19	22	24
10	19	26	27
11	24	33	34
12	30	33	37
	30	34	37
15	41	47	57
	49	52	57
	49	54	57
31	177	191	209
	177	195	209
	184	208	209
	193	200	209

Cubature along Lissajous curves: 3d case

Proposition

Consider the Lissajous curves in $[-1,1]^3$ defined by

$$\boldsymbol{\ell}_n(\theta) = (\cos(a_1\theta), \cos(a_2\theta), \cos(a_3\theta)) \ , \quad \theta \in [0, \pi] \ , \tag{7}$$

where (a_1, a_2, a_3) is an admissible triple (6).
Then, for every total-degree polynomial $p \in \mathbb{P}^3_{2n}$

$$\int_{[-1,1]^3} p(\boldsymbol{x})\, w(\boldsymbol{x}) d(\boldsymbol{x}) = \frac{1}{\pi} \int_0^{\pi} p(\boldsymbol{\ell}_n(\theta))\, d\theta \ . \tag{8}$$

($w(\boldsymbol{x})d(\boldsymbol{x})$ is the tensor product Chebyshev measure).

Proof. It suffices to prove the identity for a polynomial basis (ex: for the tensor product basis $T_\alpha(\boldsymbol{x}), |\alpha| \leq 2n$). $\square$

Polynomial exactness

Corollary

Consider $p \in \mathbb{P}^3_{2n}$, $\boldsymbol{\ell}_n(\theta)$ *and* $\nu = n \cdot \max\{a_1, a_2, a_3\} = n \cdot a_3$. *Then*

$$\int_{[-1,1]^3} p(\boldsymbol{x})\, w(\boldsymbol{x}) d\boldsymbol{x} = \sum_{s=0}^{\mu} w_s\, p(\boldsymbol{\ell}_n(\theta_s))\ , \tag{9}$$

where

$$w_s = \pi^2 \omega_s\ ,\quad s = 0, \ldots, \mu\ , \tag{10}$$

with

$$\mu = \nu\ ,\quad \theta_s = \frac{(2s+1)\pi}{2\mu+2}\ ,\quad \omega_s \equiv \frac{\pi}{\mu+1}\ ,\quad s = 0, \ldots, \mu\ , \tag{11}$$

or alternatively

$$\mu = \nu + 1\ ,\quad \theta_s = \frac{s\pi}{\mu}\ ,\quad s = 0, \ldots, \mu\ ,\ \omega_0 = \omega_\mu = \frac{\pi}{2\mu}\ ,\quad \omega_s \equiv \frac{\pi}{\mu}\ ,\quad s = 1, \ldots, \mu - 1\ . \tag{12}$$

Fourier series and Gibbs phenomenon

Multidimensional Fourier series

Take $f : \mathbb{R}^\nu \to \mathbb{R}$, $f \in L^1_{2\pi}(\mathbb{R}^\nu)$ (i.e. 2π-periodic).
The multidimensional Fourier series of f (in complex form) is

$$Sf(\boldsymbol{x}) = \sum_{\boldsymbol{n}\in\mathbb{Z}^\nu} c_{\boldsymbol{n}}(f) e_{\boldsymbol{n}}(\boldsymbol{x}) \,, \quad \boldsymbol{x} \in \mathbb{R}^\nu \,,$$

$$c_{\boldsymbol{n}}(f) = (2\pi)^{-\nu} \int_{(-\pi,\pi)^\nu} f(\boldsymbol{x}) \overline{e_{\boldsymbol{n}}(\boldsymbol{x})} \mathrm{d}\boldsymbol{x} \,.$$

and its N-partial Fourier sum is

$$S_N f(\boldsymbol{x}) = \sum_{\substack{\boldsymbol{k}\in\mathbb{Z}^\nu \\ \|\boldsymbol{k}\|_\infty \le N}} c_{\boldsymbol{k}}(f) e_{\boldsymbol{k}}(\boldsymbol{x}) \,, \quad \boldsymbol{x} \in \mathbb{R}^\nu \,, N \in \mathbb{N}$$

Remark. In applications f is often discontinuous and piecewise differentiable and

$$|c_{\boldsymbol{n}}(f)| \sim \frac{1}{\|\boldsymbol{n}\|_\infty} \quad \text{as} \quad \|\boldsymbol{n}\|_\infty \to \infty \,.$$

Multidimensional Fourier series

Take $f:\mathbb{R}^\nu \to \mathbb{R}$, $f \in L^1_{2\pi}(\mathbb{R}^\nu)$ (i.e. 2π-periodic).
The multidimensional Fourier series of f (in complex form) is

$$Sf(\boldsymbol{x}) = \sum_{\boldsymbol{n}\in\mathbb{Z}^\nu} c_{\boldsymbol{n}}(f) e_{\boldsymbol{n}}(\boldsymbol{x}), \quad \boldsymbol{x} \in \mathbb{R}^\nu ,$$

$$c_{\boldsymbol{n}}(f) = (2\pi)^{-\nu} \int_{(-\pi,\pi)^\nu} f(\boldsymbol{x}) \overline{e_{\boldsymbol{n}}(\boldsymbol{x})} \mathrm{d}\boldsymbol{x} .$$

and its N-partial Fourier sum is

$$S_N f(\boldsymbol{x}) = \sum_{\substack{\boldsymbol{k}\in\mathbb{Z}^\nu \\ \|\boldsymbol{k}\|_\infty \le N}} c_{\boldsymbol{k}}(f) e_{\boldsymbol{k}}(\boldsymbol{x}), \quad \boldsymbol{x} \in \mathbb{R}^\nu , N \in \mathbb{N}$$

Remark. In applications f is often discontinuous and piecewise differentiable and

$$|c_{\boldsymbol{n}}(f)| \sim \frac{1}{\|\boldsymbol{n}\|_\infty} \quad \text{as} \quad \|\boldsymbol{n}\|_\infty \to \infty .$$

The Gibbs phenomenon

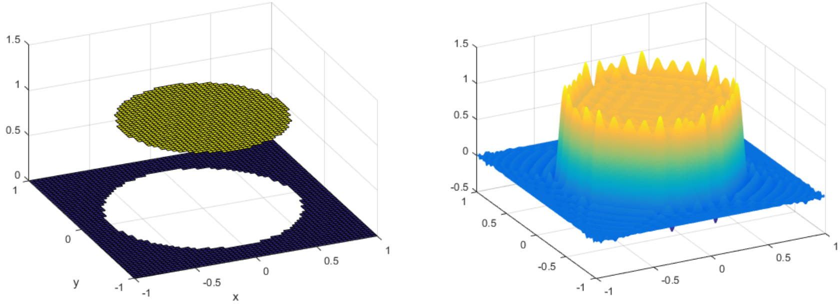

Figure: Left: original function. Right: reconstructed function

⇝ distortions and oscillations nearby the discontinuities

 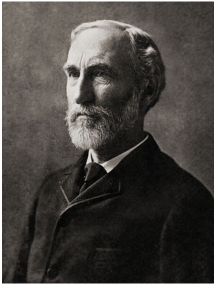

Figure: Left:Jean-Baptiste Joseph Fourier (21 March 1768 - 16 May, 1830): French mathematician and physicist Right: Josiah Willard Gibbs (February 11, 1839-April 28,1903): American engineer, chemist and physicist.

Spectral filters

Definition

$\sigma : \mathbb{R} \to \mathbb{R}$, even, is called a spectral filter of order p

1. $\sigma(\eta) \in C^{p-1}$
2. $\sigma(0) = 1$, $\sigma^{(l)}(0) = 0$ for $1 \le l \le p-1$.
3. $\sigma(\eta) = 0$ for $|\eta| \ge 1$.

Example: 1d

$$S_N^{\sigma} f(x) = \sum_{k=-N}^{N} \sigma(k/N) c_k(f) e_k(x) \ .$$

- The filter does not act on low coefficients and it affects mainly the high ones.
- Filters should be smooth functions ... Gibbs phenomenon does not disappear just cutting down the high coefficients!

Spectral filters

Definition

$\sigma : \mathbb{R} \to \mathbb{R}$, even, is called a spectral filter of order p

1. $\sigma(\eta) \in C^{p-1}$
2. $\sigma(0) = 1$, $\sigma^{(l)}(0) = 0$ for $1 \leq l \leq p-1$.
3. $\sigma(\eta) = 0$ for $|\eta| \geq 1$.

Example: 1d

$$S_N^\sigma f(x) = \sum_{k=-N}^{N} \sigma(k/N) c_k(f) e_k(x) \ .$$

- The filter does not act on low coefficients and it affects mainly the high ones.
- Filters should be smooth functions ... Gibbs phenomenon does not disappear just cutting down the high coefficients!

Filters ($|\eta| \leq 1$)

- The Fejér filter (first order)

$$\sigma(\eta) = 1 - \eta \ .$$

- The Lanczos or sinc filter (first order)

$$\sigma(\eta) = \frac{\sin(\pi\eta)}{\pi\eta} \ .$$

- The raised cosine filter (second order)

$$\sigma(\eta) = \frac{1}{2}(1 + \cos(\pi\eta)) \ .$$

- The exponential filter of order p (p even)

$$\sigma(\eta) = e^{-\alpha|\eta|^p} \ ,$$

(α is the computer's roundoff error since we want $\sigma(1) \approx 0$).

Tensor product extension

Let σ be a spectral filter and $N \in \mathbb{N}$. We consider the sequence

$$\sigma_k = \sigma(k/N)\,, \quad -N \le k \le N \tag{13}$$

and write

$$S_N^{\sigma} f(x) = \sum_{k \in \mathbb{Z}} \sigma_k c_k(f) e_k(x)\,. \tag{14}$$

Construct the tensor product pattern of ν one-dimensional filters

$$\boldsymbol{\sigma_k} = \sigma_{k_1}\sigma_{k_2}\cdots\sigma_{k_\nu} \quad , \quad -N \le k_1, k_2, ..., k_\nu \le N\,.$$

We then consider the filtered series

$$\boxed{S_N^{\boldsymbol{\sigma_k}} f(\boldsymbol{x}) = \sum_{\boldsymbol{k} \in \mathbb{Z}^\nu} \boldsymbol{\sigma_k} c_{\boldsymbol{k}}(f) e_{\boldsymbol{k}}(\boldsymbol{x})\,.} \tag{15}$$

Adaptive filtering

Remark. Classical filters acts on Fourier coefficients but do not consider physical position of discontinuities.

We can look for an adaptive filter [Tadmor, Tanner IMA J. Num. An. 2005]

$$\sigma^p(\eta) = \begin{cases} \exp\left(\frac{|\eta|^p}{\eta^2-1}\right) & |\eta| < 1 \\ 0 & |\eta| \geq 1 \end{cases} \qquad (16)$$

where $p : \mathbb{R} \to \mathbb{R}_+$ is our adaptive parameter function, $p(x)$, depending on the position x.

Adaptive filtering

Remark. Classical filters acts on Fourier coefficients but do not consider physical position of discontinuities.

We can look for an adaptive filter [Tadmor, Tanner IMA J. Num. An. 2005]

$$\sigma^p(\eta) = \begin{cases} \exp\left(\frac{|\eta|^p}{\eta^2-1}\right) & |\eta| < 1 \\ 0 & |\eta| \geq 1 \end{cases} \tag{16}$$

where $p : \mathbb{R} \to \mathbb{R}_+$ is our adaptive parameter function, $p(x)$, depending on the position x.

Main results [DeM, Erb, Marchetti 2017]

Let $\boldsymbol{\xi} = (\xi_1, \xi_2)$ be the nearest point of discontinuity with respect to $\boldsymbol{x}$ in the Euclidean norm and $d_i(x_i) = |x_i - \xi_i|$, $i = 1, 2$.

Lemma

Let σ^p as in (16). Exist positive constants M_σ, c_σ (independent of p) s.t.

$$\|\sigma^p\|_{C^p} \leq M_\sigma c_\sigma^{-p} (p!)^2 \, .$$

with $\|f\|_{C^p} = \max_{k \leq p} \|f^{(k)}\|$.

Let $\Phi_{\boldsymbol{\sigma^p}}(\boldsymbol{x}) := \frac{1}{4\pi^2} \sum_{\boldsymbol{\kappa} \in \mathbb{Z}^2} \boldsymbol{\sigma}_{\boldsymbol{\kappa}^{\boldsymbol{p}}} e_{\boldsymbol{\kappa}}(\boldsymbol{x})$ and $S_N^{\boldsymbol{\sigma^p}} f = f * \Phi_{\boldsymbol{\sigma^p}}$

Theorem (Error estimates)

Let $f : \mathbb{R}^2 \to \mathbb{R}$ be a piecewise analytic function. Setting

$$\boldsymbol{p} = (p_1(x_1), p_2(x_2)) = \left((N\eta_1^* d_1(x_1))^{1/2}, (N\eta_2^* d_2(x_2))^{1/2}\right) , \tag{17}$$

with suitably chosen η_1^* and η_2^*, then, the error $|f - S_N^{\boldsymbol{\sigma^p}} f|$ decays exponentially, away from the points of discontinuity of f.

Main results [DeM, Erb, Marchetti 2017]

Let $\boldsymbol{\xi} = (\xi_1, \xi_2)$ be the nearest point of discontinuity with respect to $\boldsymbol{x}$ in the Euclidean norm and $d_i(x_i) = |x_i - \xi_i|$, $i = 1, 2$.

Lemma

Let σ^p as in (16). Exist positive constants M_σ, c_σ (independent of p) s.t.

$$\|\sigma^p\|_{C^p} \leq M_\sigma c_\sigma^{-p} (p!)^2 \,.$$

with $\|f\|_{C^p} = \max_{k \leq p} \|f^{(k)}\|$.

Let $\Phi_{\boldsymbol{\sigma^p}}(\boldsymbol{x}) := \frac{1}{4\pi^2} \sum_{\boldsymbol{\kappa} \in \mathbb{Z}^2} \boldsymbol{\sigma}_{\boldsymbol{\kappa}^{\boldsymbol{p}}} e_{\boldsymbol{\kappa}}(\boldsymbol{x})$ and $S_N^{\boldsymbol{\sigma^p}} f = f * \Phi_{\boldsymbol{\sigma^p}}$

Theorem (Error estimates)

Let $f : \mathbb{R}^2 \to \mathbb{R}$ be a piecewise analytic function. Setting

$$\boldsymbol{p} = (p_1(x_1), p_2(x_2)) = \left((N\eta_1^* d_1(x_1))^{1/2}, (N\eta_2^* d_2(x_2))^{1/2}\right) , \qquad (17)$$

with suitably chosen η_1^* and η_2^*, then, the error $|f - S_N^{\boldsymbol{\sigma^p}} f|$ decays exponentially, away from the points of discontinuity of f.

Reconstruction algorithm

1. We consider a discontinuous and piecewise regular function f.
2. We obtain f_lissa interpolating f on the Lissajous nodes.
3. We apply a first spectral filtering process (f_filt).
4. We use an edge-detector (Canny's algorithm[Canny IEEE PAMI 1986]) on f_filt in order to find the edges and the distances we require for the adaptivity.
5. We apply the final adaptive filtering procedure, obtaining f_apt.

Results in terms of SSIM (Structural SIMilarity index) [Wang et al. IEEE TIP 2004] : product of 3 factors, liminance, contrast and structure of an image

$$SSIM(x, y) = l(x, y)^{\alpha} c(x, y)^{\beta} s(x, y)^{\gamma}$$

typically $\alpha + \beta + \gamma = 1$ (cf. Matlab manual).

Examples and parameter estimation

Example in 2D

Let $f : [-1,1]^2 \to \mathbb{R}$ be defined as

$$f(x,y) = \begin{cases} 1 & x^2 + y^2 \leq (0.6)^2 \ , \\ 0 & \text{otherwise} \ . \end{cases}$$

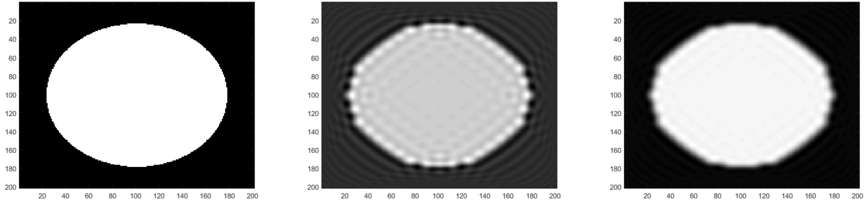

Figure: f; f_lissa, SSIM $= 0.5122$; f_filt, SSIM $= 0.8232$

Modification of the adaptive parameter: heuristic

$$p_1 = (\eta N_1 d_1)^{1/2}\,,\; p_2 = (\eta N_2 d_2)^{1/2}\,. \tag{18}$$

We look for a unique parameter $p = p_1 = p_2$ which depends on the Euclidean distance

$$d(\boldsymbol{x}) = \|\boldsymbol{x} - \boldsymbol{\xi}\| = \sqrt{d_1^2 + d_2^2}\,. \tag{19}$$

Then, we take

$$N = \sqrt{N_1^2 + N_2^2}\,, \tag{20}$$

and modify the initial parameters in

$$p_1 = (\eta N d_1)^{1/2} \quad , \quad p_2 = (\eta N d_2)^{1/2}\,. \tag{21}$$

getting

$$\boxed{p = \sqrt{p_1^4 + p_2^4} = \eta N d(\boldsymbol{x})} \tag{22}$$

Modification of the adaptive parameter: heuristic

$$p_1 = (\eta N_1 d_1)^{1/2}\,,\; p_2 = (\eta N_2 d_2)^{1/2}\,. \tag{18}$$

We look for a unique parameter $p = p_1 = p_2$ which depends on the Euclidean distance

$$d(\boldsymbol{x}) = \|\boldsymbol{x} - \boldsymbol{\xi}\| = \sqrt{d_1^2 + d_2^2}\,. \tag{19}$$

Then, we take

$$N = \sqrt{N_1^2 + N_2^2}\,, \tag{20}$$

and modify the initial parameters in

$$p_1 = (\eta N d_1)^{1/2} \quad , \quad p_2 = (\eta N d_2)^{1/2}\,. \tag{21}$$

getting

$$\boxed{p = \sqrt{p_1^4 + p_2^4} = \eta N d(\boldsymbol{x})} \tag{22}$$

Example in 2D (cont.)

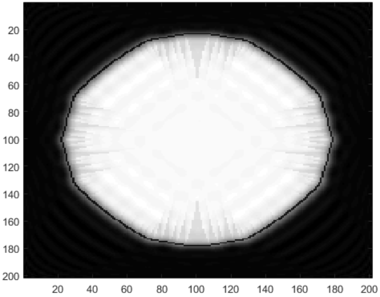

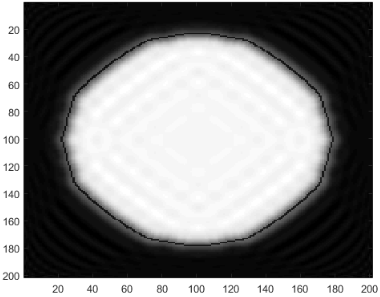

Figure: f_apt; $SSIM = 0.6592$; $f^{\star}\_apt$, $SSIM = 0.6120$

Modification of the adaptive parameter (cont.)

Consider the function $\varphi : [0, +\infty) \to [0, +\infty)$ such that

- $\varphi(0) = 0$.
- φ is a continuous increasing function in $[0, +\infty)$.
- φ has a saturation property, i.e. exists $\epsilon > 0$ such that

$$\varphi(x) \geq x \,, \quad x \in [0, \epsilon]$$

Conjecture

There exists at least one function φ for which

$$p = \eta N \varphi(d(\boldsymbol{x}))$$

such that we can improve the reconstruction

Modification of the adaptive parameter (cont.)

Let

$$\varphi_\beta(x) = x^\beta \ ,$$

where $0 < \beta < 1$. Then we can define a new parameter

$$p_\beta = \eta N(d(\boldsymbol{x}))^\beta$$

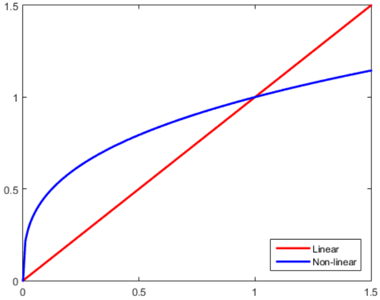

Example in 2D (cont.)

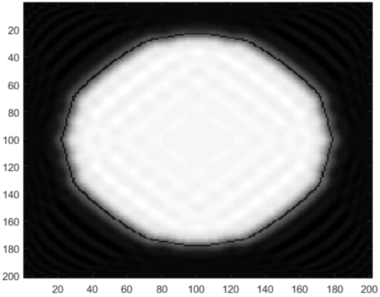

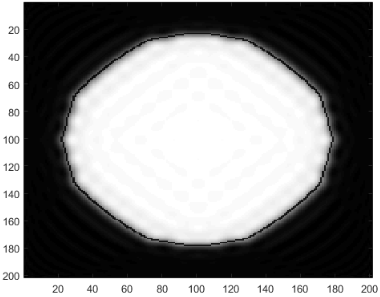

Figure: $f^{\star}\_apt$, $SSIM = 0.6120$; $f^{1/4}\_apt$, $SSIM = 0.7073$

More numerical results

Consider the functions defined in $[-1,1]^2$.

$$f_1(x,y) = \begin{cases} 2 & |x| \le 0.5\ ,\ |y| \le 0.5\ , \\ 1 & -0.8 \le x \le -0.65\ ,\ |y| \le 0.8\ , \\ 0.5 & 0.65 \le x \le 0.8\ ,\ |y| \le 0.2\ , \\ 0 & \text{otherwise}\ . \end{cases}$$

$$f_2(x,y) = \begin{cases} 2 & (x+0.4)^2 + (y+0.4)^2 \le 0.4^2\ , \\ 1.5 & (x-0.5)^2 + (y-0.5)^2 \le 0.3^2\ , \\ 1 & (x-0.5)^2 + (y+0.5)^2 \le 0.2^2\ , \\ 0.5 & (x+0.5)^2 + (y-0.5)^2 \le 0.1^2\ , \\ e^{-(x^2+y^2)} & \text{otherwise}\ . \end{cases}$$

More numerical results (cont.)

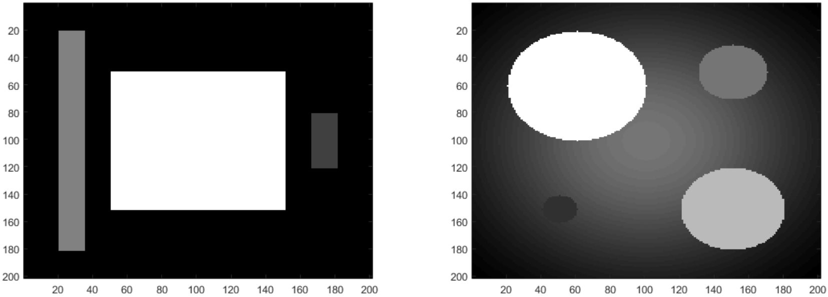

Figure: The functions f_1 and f_2

More numerical results: f_1

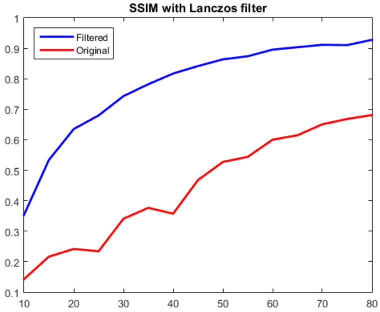

Figure: Left: using the Lanczos filter. Right: after the adaptive filter.

More numerical results: f_1 (cont.)

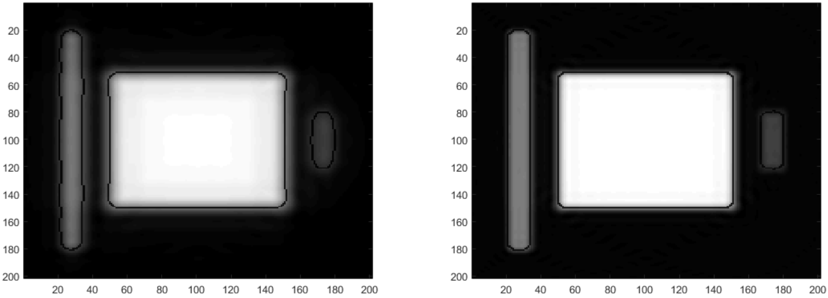

Figure: $n = 25$, $n = 40$

More numerical results: f_2

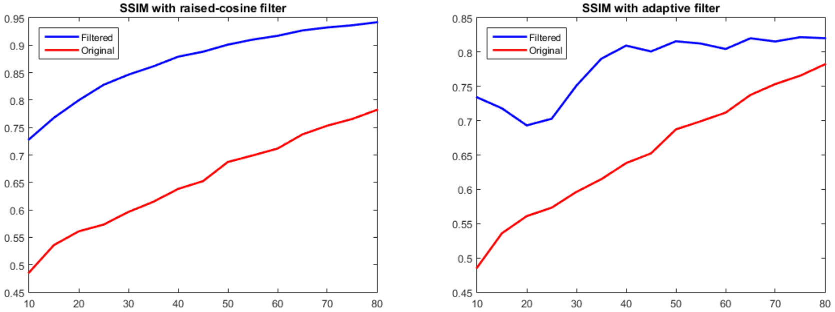

Figure: Left: using the raised cosine filter. Right: after the adaptive filter.

More numerical results: f_2 (cont.)

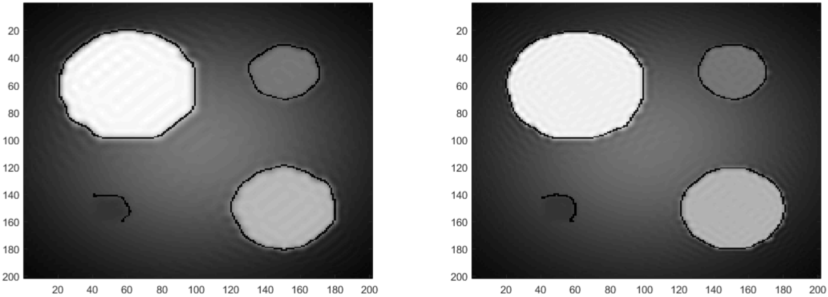

Figure: $n = 45$, $n = 65$

MPI application

MPI applications

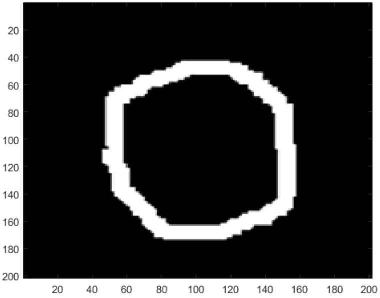

Figure: Phantoms discretized by 201×201 points.

MPI applications (cont.)

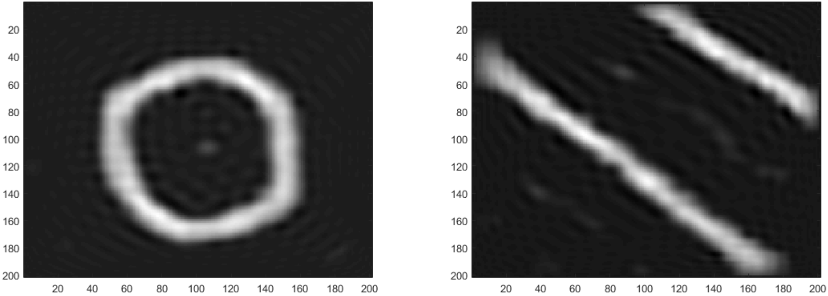

Figure: Reconstruction along the Lissajous curve. Left: $SSIM = 0.665$; Right:$SSIM = 0.616$

Remark. Reconstruction has been done using the nodes $LS^{(66,64)}$ of a non-degenerate Lissajous curve $\gamma_2^{(33,32)}$.

MPI applications (cont.)

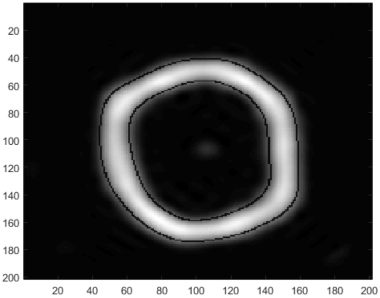

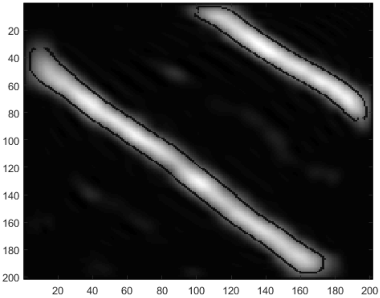

Figure: Adaptive filtering using raised cosine and parameters $\beta = 1/4$, $\eta = 0.0159$. Left: SSIM=0.701; Right: SSIM=0.649

Example in 3D

We considered f on $[-1,1]^3$ defined as

$$f(x,y,z) = \begin{cases} 1 & x^2+y^2+z^2 \le (0.6)^2 \ , \\ 0 & \text{otherwise} \ . \end{cases}$$

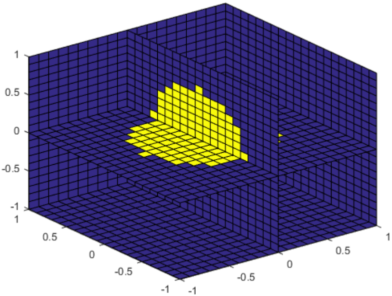

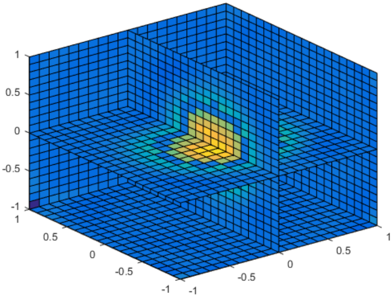

Figure: The original function f: SSIM=0.33 on the Lissajous curve $\gamma_{(14,16,19)}$ [BDeMV IMA J. NA 2017] sampled on 165 pts , i.e. with degree $m = 8$.

Summary

1. Lissajous sampling in 2D and 3D
2. Modification of the Chebfun package
3. Spectral filtering and Gibbs phenomenon
4. Adaptive filtering

References

1. Bos M., De Marchi S. and Vianello M.: Trivariate polynomial approximation on Lissajous curves. *IMA J. Num. Anal.* (2017), online.
2. S. De Marchi, W. Erb and F. Marchetti: Spectral filtering for the reduction of the Gibbs phenomenon of polynomial approximation methods on Lissajous curves with applications in MPI, submitted 2017.
3. Dencker P., and Erb W.: Multivariate polynomial interpolation on Lissajous-Chebyshev nodes. *arXiv:1511.04564 [math.NA]* (2015).
4. Erb W., Kaethner C., Ahlborg M. and Buzug T.M.: Bivariate Lagrange interpolation at the node points of non-degenerate Lissajous nodes. *Numerische Mathematik*, 133(4):685–705, 2016.
5. Erb W., Kaethner C., Dencker P., and Ahlborg M.: A survey on bivariate Lagrange interpolation on Lissajous nodes. *Dolomites Res. Notes Approx. 8* (2015), 23–36.
6. Knopp T. and Buzug T. M.: Magnetic Particle Imaging. *Springer* (2012).
7. Knopp T., Biederer S., Sattel T., Weizenecker J., Gleich B., Borgert J. and Buzug T. M.: Trajectory analysis for magnetic particle imaging. *Phys. Med. Biol. 54(2)* (2009), 385–397.
8. Marchetti F.: Spectral filtering for the resolution of the Gibbs phenomenon in MPI applications by Lissajous sampling, *Master thesis, University of Padova* (2016). `http://tesi.cab.unipd.it/54084/`

DRWA17

Dolomites Research Week on Approximation 2017
September 4-8, Alba di Canazei - Italy
`http://events.math.unipd.it/drwa17/`

Tutorial on
Approximation methods in Magnetic Particle Imaging (MPI)
Wolfgang Erb (Hawaii)

Danke
Thanks
Grazie!

see you next year ... in Bernried